NEAT1 silencing alleviates pulmonary arterial smooth muscle cell migration and proliferation under hypoxia through regulation of miR-34a-5p/KLF4 *in vitro*

XIULI DOU[1], YUXIAO MA[1], YIJIE QIN[1], QINGLIN DONG[1], SHOUWEI ZHANG[2], RUI TIAN[3] and MINGYU PAN[4]

Departments of [1]Emergency and [2]Medical, The People's Hospital of Rizhao, Rizhao, Shandong 276800; [3]Department of Cardiology, Beijing Anzhen Hospital, Capital Medical University, Beijing 100029; [4]Department of Cardiology, The People's Hospital of Rizhao, Rizhao, Shandong 276800, P.R. China

Received October 28, 2020; Accepted March 29, 2021

DOI: 10.3892/mmr.2021.12389

Abstract. Pulmonary arterial hypertension (PAH) is a severe vascular disease that adversely affects patient health and can be life threatening. The present study aimed to investigate the detailed role of nuclear paraspeckle assembly transcript 1 (NEAT1) in PAH. Using RT-qPCR, the expression levels of NEAT1, microRNA (miR)-34a-5p, and Krüppel-like factor 4 (KLF4) were detected in both hypoxia-treated pulmonary arterial smooth muscle cells (PASMCs) and serum from PAH patients. Then, the interactions among miR-34a-5p, NEAT1, and KLF4 were evaluated by dual-luciferase reporter assay. The detailed role of the NEAT1/miR-34a-5p/KLF4 axis in PAH pathogenesis was further explored using MTT, Transwell, and western blot assays. The results revealed that NEAT1 targeted miR-34a-5p and miR-34a-5p targeted KLF4. In hypoxia-treated PASMCs and serum from PAH patients, high NEAT1 and KLF4 expression levels and low miR-34a-5p expression were observed. The proliferation and migration of hypoxia-treated PASMCs were reduced by transfection with sh-NEAT1 or miR-34a-5p mimics. The suppressive effects of NEAT1 knockdown on the proliferation and migration of hypoxia-treated PASMCs were reversed by knock down of miR-34a-5p expression and increased KLF4 expression. NEAT1 was not only highly expressed in the serum of PAH patients but its silencing also alleviated PAH by regulating miR-34a-5p/KLF4 *in vitro*. The present study highlighted a potential new therapeutic target and diagnostic biomarker for PAH.

Correspondence to: Dr Mingyu Pan, Department of Cardiology, The People's Hospital of Rizhao, 126 Tai'an Road, Rizhao, Shandong 276800, P.R. China
E-mail: panmingyu314@163.com

Key words: pulmonary arterial hypertension, long non-coding RNA nuclear paraspeckle assembly transcript 1, microRNA-34a-5p, Krüppel-like factor 4

Introduction

Pulmonary arterial hypertension (PAH) typically originates from hyperplasia of pulmonary arterial smooth muscle cells (PASMCs) (1,2). Under normal physiological conditions, PASMCs are quiescent and contractile (3). However, under hypoxia, the phenotype of PASMCs can switch, leading to excessive proliferation and migration (4,5), eventually resulting in pulmonary vasoconstriction and vascular remodelling (6). Therefore, exploring the mechanism by which hypoxia induces the proliferation and migration of PASMCs is vital for treating PAH in the clinic.

Various long non-coding RNAs (lncRNAs) have been revealed to promote the development of PAH (7-9). For example, Zhang *et al* reported that HOXA-AS3 was overexpressed in both the lung vasculature of monocrotaline (MCT)-treated mice and PASMCs from patients with PAH (7). In addition, Wang *et al* detected high MALAT1 expression in PAH tissues and PASMCs (8). Yang *et al* demonstrated that hypoxia increased the expression of taurine upregulated gene 1 (TUG1) in the pulmonary artery (PA) of a PAH mouse model, whereas silencing of TUG1 markedly decreased the hyperproliferation of PASMCs (9). Additionally, inhibition of NEAT1 has been reported to suppress the proliferation and migration of numerous human cancers, including pancreatic (10), breast (11), non-small cell lung (12) and colorectal cancers (13). More relevant to the present study, Ahmed *et al* (14) demonstrated that knockout of NEAT1 increased the levels of contractile proteins in vascular smooth muscle (VSM) cells (VSMCs), allowing them to maintain their contractile status and ultimately inhibit vascular hyperplasia. However, the possible role of NEAT1 in hypoxia-treated PASMCs has yet to be elucidated.

Notably, the expression levels of some microRNAs (miRNAs) are reduced in lung vascular tissues and/or PASMCs, which are likely involved in the progression of PAH (15-17). For instance, downregulation of miR-98 was revealed to enhance the proliferation-promoting effect of hypoxia on PASMCs (15). In an MCT-induced rat model, low miR-140-5p expression was observed, which suppressed PAH by targeting TNF-α (16). MiR-182-3p was downregulated in patients with

PAH as well as in hypoxia-stimulated model mice/rats, and miR-182-3p upregulation had a distinct antiproliferative effect on PASMCs (17). Notably, a recent study revealed that miR-34a was expressed at low levels in the PA of rats, and it inhibited the proliferation of PASMCs by targeting PDGFRA (18). lncRNAs can modulate the function of miRNAs by sponging them and thus acting as competing endogenous RNAs. Whether miR-34a-5p interacts with NEAT1 and whether this interaction is involved in the pathogenesis of PAH needs to be further investigated.

Krüppel-like factor 4 (KLF4), a member of the KLF family of zinc-finger transcription factors (19), was reported to be associated with the progression of PAH (20,21). Sun *et al* (20) revealed that KLF4 expression was significantly increased in remodelled pulmonary arteries from a rat model of pulmonary vascular remodelling, and downregulation of KLF4 suppressed the proliferation and migration of PASMCs. Liang *et al* (21) demonstrated that increased KLF4 expression promoted the migration and cell cycle progression of pulmonary artery endothelial cells. In addition, KLF4 was revealed to be an oncogene that is regulated by miRNAs to promote tumour progression in various human cancers, such as miR-148-3p/miR-152-3p in prostate cancer (22), miR-32 in gastric cancer (23), and miR-543 in colorectal cancer (24). Most relevant to our research, a recent study revealed that miR-182-3p mediated vascular remodelling in PAH by targeting KLF4 (17). However, whether regulation of KLF4 by miR-34a-5p is involved in PAH and the underlying mechanism have yet to be elucidated.

In the present study, the possible roles of NEAT1, miR-34a-5p, and KLF4 in the pathogenesis of PAH *in vitro* were investigated, which will provide novel insights into the diagnosis and treatment of PAH.

Materials and methods

Serum samples. From January 2018 to December 2019, serum samples were collected from 25 patients (19 females and 6 males; age range, 21-48 years old; mean age, 35.04±8.44 years old) with PAH and 25 healthy volunteers (19 females and 6 males; age range, 21-50 years old; mean age, 34.96±8.58 years old) in The People's Hospital of Rizhao (Shandong, China). Patients with ≥1 of the following conditions were excluded: i) Other types of PAH, including familial PAH; ii) heart diseases, including left ventricular diseases and acute heart failure; iii) chronic respiratory disorders, including chronic obstructive pulmonary disease; iv) diabetes mellitus; and v) prior targeted therapy. No patients had received prior medical treatment. The inclusion criteria for healthy controls were that subjects must be age- and sex-matched with patients and absent of any diseases when enrolled. The study was approved by the Ethics Committee of The People's Hospital of Rizhao, and written informed consent was obtained from all study participants. The collected serum samples were centrifuged at 450 x g for 20 min at 20˚C and immediately stored at -80˚C until use.

Cell culture, hypoxia stimulation, and transfection. Human PASMCs (BioVector NTCC, Inc.) were cultured in Dulbecco's modified Eagle's medium (DMEM; Invitrogen; Thermo Fisher Scientific, Inc.) containing 10% foetal bovine serum (FBS; Gibco; Thermo Fisher Scientific, Inc.) and 0.1% penicillin/streptomycin (ScienCell Research Laboratories, Inc.) at 37˚C with 5% CO_2. The cells were divided into two groups: The hypoxia group, which was treated with 5% CO_2 and 95% N_2 at 37˚C for 48 h, and the normoxia group, which was treated with 5% CO_2, 21% O_2, and 74% N_2 at 37˚C for 48 h. The short hairpin (sh) RNA targeting NEAT1 (sh-NEAT1-1, 5'-GCCAUCAGCUUUGAAUAAAUU-3'; shNEAT1-2, 5'-GGUGUUAUCAAGUGAAUUAUU-3') and negative control (sh-NC, 5'-UUCUCCGAACGUGUCACGU-3') were obtained from Shanghai Transheep Bio-Tech Co., Ltd. The KLF4 overexpression vector (pcDNA-KLF4), overexpression negative control (pcDNA-NC), miR-34a-5p mimics (5'-GAUGGACGUGCUUGUCGUGAAAC-3') and non-targeting mimics control (miR-NC, 5'-UUCUCCGAACGUGUCACGUTT-3'), miR-34a-5p inhibitor (5'-CUACCUGCACCAACAGCACUU-3'), and non-targeting inhibitor control (inhibitor NC, 5'-CAGUACUUUUGUGUAGUACAA-3') were obtained from Beina Biology. All the above agents (all at 20 nM) were co-transfected into hypoxia-treated PASMCs using the Lipofectamine® RNAiMAX kit (Invitrogen; Thermo Fisher Scientific, Inc.) at 37˚C. Subsequently, 48 h after transfection, PASMCs were harvested to perform further experiments.

Reverse transcription-quantitative (RT-q)PCR. Total RNA was extracted from the serum of patients with PAH, healthy volunteers, and PASMCs using the Total RNA Extraction Kit (Beijing Solarbio Science & Technology Co., Ltd.). According to the manufacturer's instructions, cDNA was synthesized using the First-Strand cDNA Synthesis Kit (APExBIO Technology), and RT-qPCR was performed with SYBR Green FAST Mastermix (Qiagen GmbH). The following thermocycling conditions were used for the qPCR: Initial denaturation at 95˚C for 3 min followed by 40 cycles at 95˚C for 15 sec, annealing at 60˚C for 30 sec, elongation at 72˚C for 1 min, and a final extension at 72˚C for 5 min. Experimental results were quantified by the $2^{-\Delta\Delta Cq}$ method (25). The expression levels of NEAT1 and KLF4 were normalised to *GAPDH*, and the expression level of miR-34a-5p was normalised to *U6*. The respective sequences of primers were as follows: NEAT1 forward, 5'-GGGGCCACATTAATCACAAC-3' and reverse, 5'-CAGGGTGTCCTCCACCTTTA-3'; miR-34a-5p forward, 5'-GGGGTGGCAGTGTCTTAGC-3' and reverse, 5'-CAGTGCGTGTCGTGGAGT-3'; KLF4 forward, 5'-TTCCCATCTCAAGGCACACC-3' and reverse, 5'-CATGTGTAAGGCGAGGTGGT-3'; GAPDH forward, 5'-CCAGGTGGTCTCCTCTGA-3' and reverse, 5'-GCTGTAGCCAAATCGTTGT-3'; and U6 forward, 5'-CTCGCTTCGGCAGCACA-3' and reverse, 5'-AACGCTTCACGAATTTGCGT-3'.

3-(4,5-Dimethyl-2-thiazolyl)-2, 5-diphenyl-2-h-tetrazolium bromide (MTT) assay. Anoxic and transfected PASMCs ($2x10^3$) were cultured in 96-well plates for 48 h at 37˚C. Then, MTT (Nanjing Keygen Biotech Co., Ltd.) was added, and the cells were incubated for 2 h at 37˚C. Thereafter, 100 μl dimethyl sulfoxide was added to dissolve the formazan. Cell viability was assessed by measuring the absorbance at an optical density of 450 nm using a microplate reader (Molecular Devices, LLC).

Transwell migration assay. The hypoxia-treated and transfected PASMCs ($2x10^4$) were resuspended in 200 μl of serum-free medium and then plated into the upper chambers of each Transwell apparatus (8 μm pore size; BD Biosciences). A total of 600 μl of medium containing 10% FBS was added to the lower chambers followed by incubation at 37˚C for 48 h. Subsequently, the cells in the upper chambers were wiped off using a cotton swab and those adhering to the lower chambers were fixed with 4% paraformaldehyde for 1 h and stained with 0.5% crystal violet [TCI (Shanghai) Development Co., Ltd.] at 37˚C for 30 min. Stained cells were imaged using an inverted light microscope (magnification, x400; Olympus Corporation) and analysed with ImageJ software (version 1.46, National Institutes of Health).

Western blotting. Hypoxia-treated and transfected PASMCs were lysed with RIPA buffer (Beyotime Institute of Biotechnology) to extract total protein. The protein concentration was detected by the BCA Protein Assay kit. Then, a total of 50 μg of protein/lane was separated by 10% sodium dodecyl sulfate-polyacrylamide gel electrophoresis and then transferred onto polyvinylidene fluoride membranes. Following blocking with 5% skimmed milk for 2 h at 25˚C, the membranes were incubated with the following primary antibodies: PCNA (1:1,000; Abcam; cat. no. ab92552), MMP2 (1:1,000; Abcam; cat. no. ab92536), α-smooth muscle actin (α-SMA; 1:1,000; Abcam; cat. no. ab5694), total caspase-3 (t-caspase-3; 1:1,000; Abcam; cat. no. ab32351), cleaved caspase-3 (c-caspase-3; 1:1,000; Abcam; cat. no. ab2302), KLF4 (1:1,000; Abcam; cat. no. ab215036), and GAPDH (1:1,000; Abcam; cat. no. ab215036) at 4˚C overnight, and then with the secondary antibody, HRP-conjugated anti-rabbit IgG (1:3,000; Abcam; cat. no. ab6721) for 1 h at 37˚C. The immunoblots were visualised using an ECL detection kit (Thermo Fisher Scientific, Inc.) under Gel-Pro analyzer (version 4.0; Media Cybernetics, Inc.).

Dual luciferase reporter (DLR) assay. The targeting relationship between NEAT1 and miR-34a-5p was analysed using the StarBase software (version 2.0; http://starbase.sysu.edu.cn). Additionally, the targeting relationship between miR-34a-5p and KLF4 was predicted using TargetScan software (release 7.2; http://www.targetscan.org/vert_72/). Fragments of NEAT1/KLF4 containing the miR-34a-5p binding site [wild-type (wt) and mutated (mut)] were inserted into the pGL3 vector (Promega Corporation) to generate recombinant luciferase reporter plasmids. PASMCs in 96-well plates (2,000 cells/well) were co-transfected with either miR-34a-5p mimics or miR-NC and either wt or mut NEAT1/KLF4 using Lipofectamine 3000 (Invitrogen; Thermo Fisher Scientific, Inc.). Following transfection for 48 h at 37˚C, luciferase activity was analysed using the DLR gene assay system (Promega Corporation). The activity of firefly luciferase was normalized to that of *Renilla* luciferase.

Statistical analysis. All experiments were performed in triplicate, and each experiment was repeated three times. Data were analysed using SPSS 23.0 software (IBM Corp.) and presented as the mean ± SD. Comparisons between two groups were performed using unpaired t-test, and comparisons among multiple groups were performed using ANOVA, followed by Tukey's multiple comparison test. Pearson's correlation analysis was used to assess the linear correlation of serum concentrations in patients with PAH. $P<0.05$ was considered to indicate a statistically significant difference.

Results

Low expression of lncRNA NEAT1 protects against PAH in vitro. It was initially observed that the expression of NEAT1 was significantly increased in hypoxia-treated PASMCs when compared to its expression levels in normoxic PASMCs (Fig. 1A; $P<0.01$). Given that NEAT1 was overexpressed in hypoxia-treated PASMCs, NEAT1 was knocked down in hypoxia-treated PASMCs by transfecting sh-NEAT1-1/-2 to further explore the effects of NEAT1 on PAH *in vitro*. An analysis of transfection efficiency revealed a decrease in NEAT1 expression in transfected cells (Fig. 1B; $P<0.01$). sh-NEAT1-1-transfected cells were selected for further study due to their relatively low NEAT1 expression. An MTT assay was performed to measure cell viability, which indicated that transfection of sh-NEAT1 reversed the positive effect of hypoxia on the viability of PASMCs (Fig. 1C; $P<0.01$). The Transwell assay produced similar data, revealing that hypoxia treatment significantly promoted the migration of PASMCs, which was reversed by transfection with sh-NEAT1 (Fig. 1D; $P<0.01$). To further verify the effects of sh-NEAT1 on the proliferation and migration of hypoxia-treated PASMCs, a western blot assay was performed, which demonstrated that knock down of NEAT1 expression markedly reduced the hypoxia-induced increases in the protein levels of PCNA (a proliferation-related protein) (26) and MMP2 (a migration-related protein) (27) (Fig. 1E; $P<0.01$). It was also determined that hypoxia treatment significantly reduced the level of α-SMA (a marker of VSM-specific contraction) (28), and the ratio of c-caspase-3/t-caspase-3 (a pro-apoptosis-related protein) (29) compared to the normoxic group, indicating that more contractile PASMCs were converted to a proliferative phenotype. However, these inhibitory effects were reversed by transfection with sh-NEAT1-1 (Fig. 1F; $P<0.01$).

NEAT1 sponges miR-34a-5p. An underlying binding site between NEAT1 and miR-34a-5p was revealed using StarBase (Fig. 2A). Then a DLR assay was conducted to assess the role of this binding site and miR-34a-5p on NEAT1 expression, which yielded an interesting result; the luciferase activity of the wt NEAT1 reporter was decreased by transfection of miR-34a-5p mimics, whereas the luciferase activity of the NEAT1 mut reporter was unaffected (Fig. 2B; $P<0.01$). This result confirmed the relationship between NEAT1 and miR-34a-5p. Additionally, the expression of miR-34a-5p in PASMCs was increased by transfection of sh-NEAT1 (Fig. 2C; $P<0.01$), indicating an inverse relationship between them.

High expression of miR-34a-5p has suppressive effects on PAH in vitro. The expression of miR-34a-5p in PASMCs under hypoxia was evaluated by RT-qPCR. The results of RT-qPCR revealed that, when compared to PASMCs under normoxia, the expression of miR-34a-5p was reduced in hypoxia-treated PASMCs (Fig. 3A; $P<0.01$). To explore the possible functions

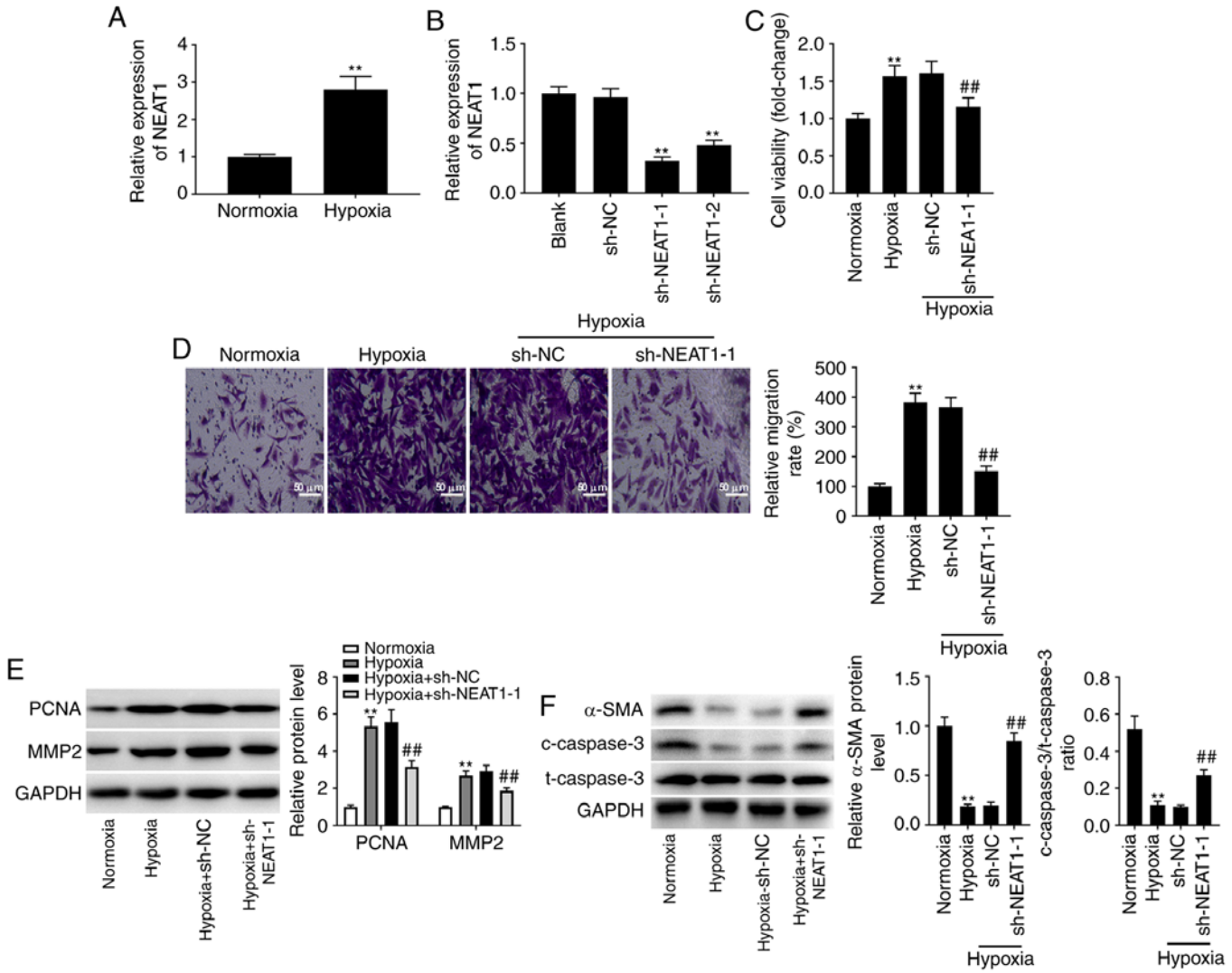

Figure 1. Low expression of lncRNA NEAT1 protects against PAH *in vitro*. (A) The expression of NEAT1 in hypoxia-induced PASMCs was detected by RT-qPCR. **P<0.01 vs. the normoxia PASMC group. (B) The expression of NEAT1 after transfection of sh-NEAT1-1/-2/NC in hypoxia-induced PASMCs was detected by RT-qPCR. **P<0.01 vs. the sh-NC group. (C) The viability (OD_{450}) of hypoxia-induced PASMCs was measured by MTT assay. (D) The migration of hypoxia-induced PASMCs was measured by Transwell assay. Scale bar, 50 μm. (E) The protein levels of PCNA and MMP2 in hypoxia-induced PASMCs after transfection of sh-NEAT1-1/NC were detected by western blotting. (F) The protein levels of α-SMA, and c-caspase-3/t-caspase-3 ratio in hypoxia-induced PASMCs after transfection of sh-NEAT1-1/NC was detected by western blotting. **P<0.01 vs. the normoxia PASMC group; ##P<0.01 vs. the hypoxia + sh-NC group. lncRNA, long non-coding RNA; NEAT1, nuclear paraspeckle assembly transcript 1; PAH, pulmonary arterial hypertension; PASMCs, pulmonary arterial smooth muscle cells; sh-, short hairpin; NC, negative control; RT-qPCR, reverse transcription-quantitative PCR; MTT, 3-(4,5-dimethyl-2-thiazolyl)-2, 5-diphenyl-2-h-tetrazolium bromide.

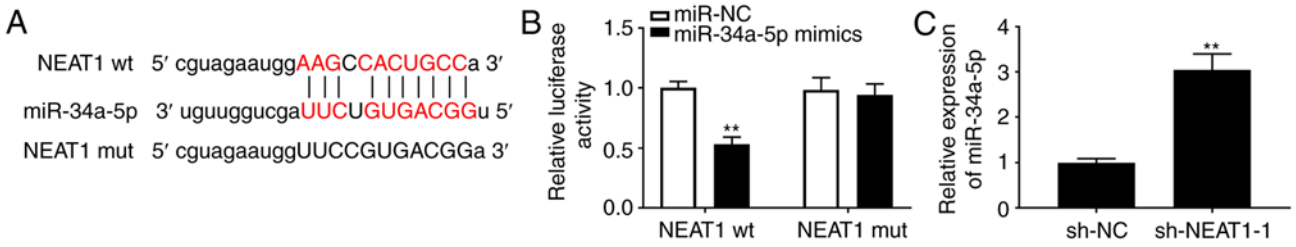

Figure 2. NEAT1 sponges miR-34a-5p. (A) The complementary binding site of NEAT1 and miR-34a-5p was predicted by StarBase software. (B) The luciferase activity in PASMCs co-transfected with pGL3-NEAT1 wt/pGL3-NEAT1 mut and miR-34a-5p mimics/NC was determined by dual luciferase reporter assay. **P<0.01 vs. the miR-NC group. (C) The expression of miR-34a-5p after transfection of sh-NEAT1-1/NC in hypoxia-induced PASMCs was detected by reverse transcription-quantitative PCR. **P<0.01 vs. the sh-NC group. NEAT1, nuclear paraspeckle assembly transcript 1; miR-34a-5p, microRNA-34a-5p; PASMCs, pulmonary arterial smooth muscle cells; wt, wild-type; mut, mutated; NC, negative control; sh-, short hairpin.

of miR-34a-5p in the pathogenesis of PAH *in vitro*, miR-34a-5p mimics or inhibitor was transfected into hypoxia-treated PASMCs. As anticipated, miR-34a-5p expression was increased by miR-34a-5p mimics, whereas it was reduced by

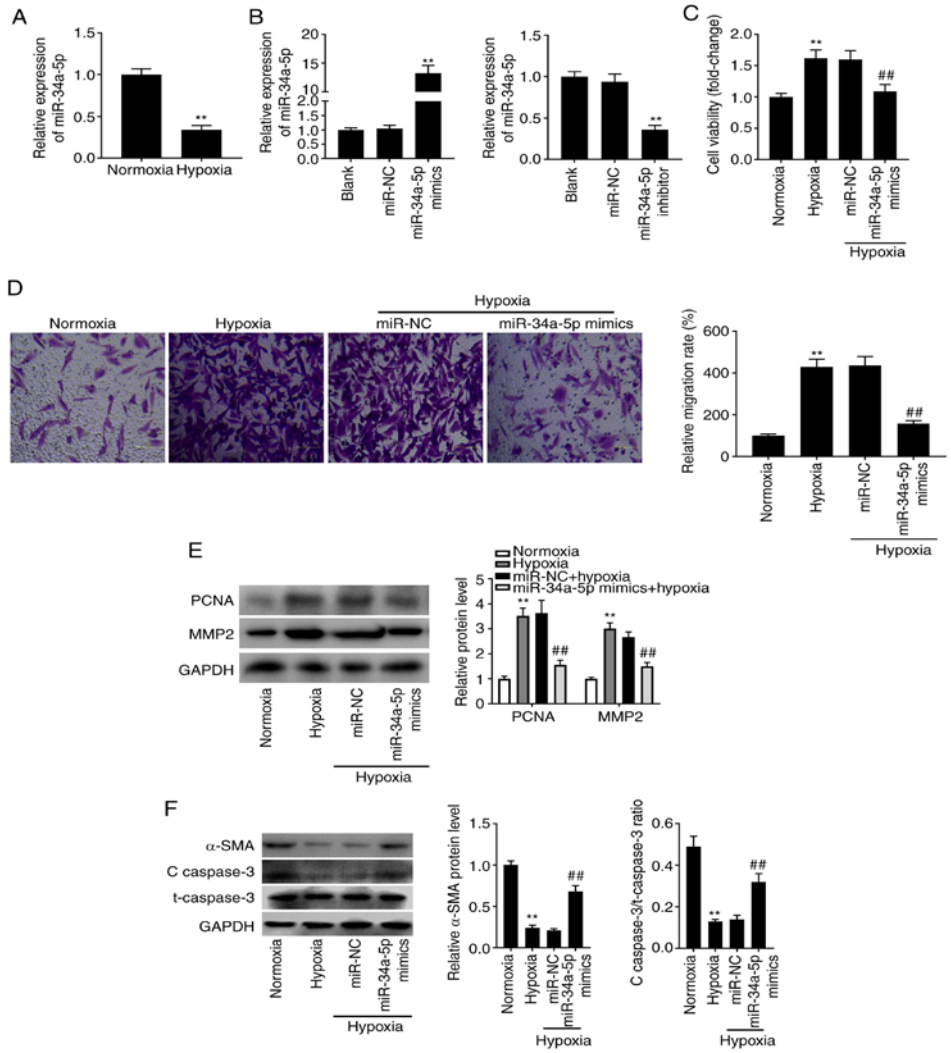

Figure 3. High expression of miR-34a-5p plays a suppressive role in PAH *in vitro*. (A) The expression of miR-34a-5p in hypoxia-induced PASMCs was detected by RT-qPCR. **P<0.01 vs. the normoxia PASMC group. (B) The expression of miR-34a-5p after transfection of miR-34a-5p mimics/inhibitor in hypoxia-induced PASMCs was detected by RT-qPCR. **P<0.01 vs. the miR-NC group. (C) The viability (OD_{450}) of hypoxia-induced PASMCs was measured by MTT assay. (D) The migration of hypoxia-induced PASMCs was measured by Transwell assay. Scale bar, 50 μm. (E) The protein levels of PCNA and MMP2 in hypoxia-induced PASMCs after transfection of miR-34a-5p mimics/NC were detected by western blotting. (F) The protein levels of α-SMA, and c-caspase-3/t-caspase-3 ratio in hypoxia-induced PASMCs after transfection of miR-34a-5p mimics/NC were detected by western blotting. **P<0.01 vs. the normoxia PASMC group; $^{\#\#}$P<0.01 vs. the hypoxia + miR-NC group. miR-34a-5p, microRNA-34a-5p; PAH, pulmonary arterial hypertension; PASMCs, pulmonary arterial smooth muscle cells; RT-qPCR, reverse transcription-quantitative PCR; NC, negative control; MTT, 3-(4,5-dimethyl-2-thiazolyl)-2, 5-diphenyl-2-h-tetrazolium bromide; c-, cleaved; t-, total.

the miR-34a-5p inhibitor (Fig. 3B; P<0.01). The increases in proliferation (Fig. 3C; P<0.01) and migration (Fig. 3D; P<0.01) of PASMCs induced by hypoxia were partly reversed by overexpression of miR-34a-5p. Western blotting revealed that transfection of miR-34a-5p mimics significantly reduced the hypoxia-induced increases in PCNA and MMP2 protein levels (Fig. 3E; P<0.01), which further confirmed the results of the MTT and Transwell assays. Concurrently, overexpression of miR-34a-5p increased the protein levels of α-SMA, and the c-caspase-3/t-caspase-3 ratio (Fig. 3F; P<0.01).

MiR-34a-5p targets KLF4. TargetScan predicted a potential binding site for miR-34a-5p in KLF4 (Fig. 4A; P<0.01). In addition, a DLR assay revealed lower luciferase activity in KLF4-wt/miR-34a-5p-mimic-transfected cells than in KLF4-wt/miR-NC-transfected cells (Fig. 4B; P<0.01), indicating a strong association between KLF4 and miR-34a-5p. Western blotting was performed to further examine the interactions among NEAT1, miR-34a, and KLF4 in hypoxia-treated PASMCs. It was determined that KLF4 protein levels were reduced by transfection of miR-34a-5p mimics (Fig. 4C; P<0.01) as well as by transfection of sh-NEAT1-1, whereas transfection of a miR-34a-5p inhibitor reversed the suppressive effect of sh-NEAT-1 on KLF4 levels (Fig. 4D; P<0.05).

Knockdown of NEAT1 slows the process of PAH by sponging miR-34a-5p and downregulating KLF4. As presented in Fig. 5A, KLF4 protein levels were increased in hypoxia-treated PASMCs but not in cells under normoxia (P<0.01). pcDNA-KLF4 was transfected into hypoxia-treated PASMCs and the transfection efficiency was first evaluated. Transfection of pcDNA-KLF4 was determined to be successful due to the significant increase in KLF4 levels (Fig. 5B; P<0.01). Using

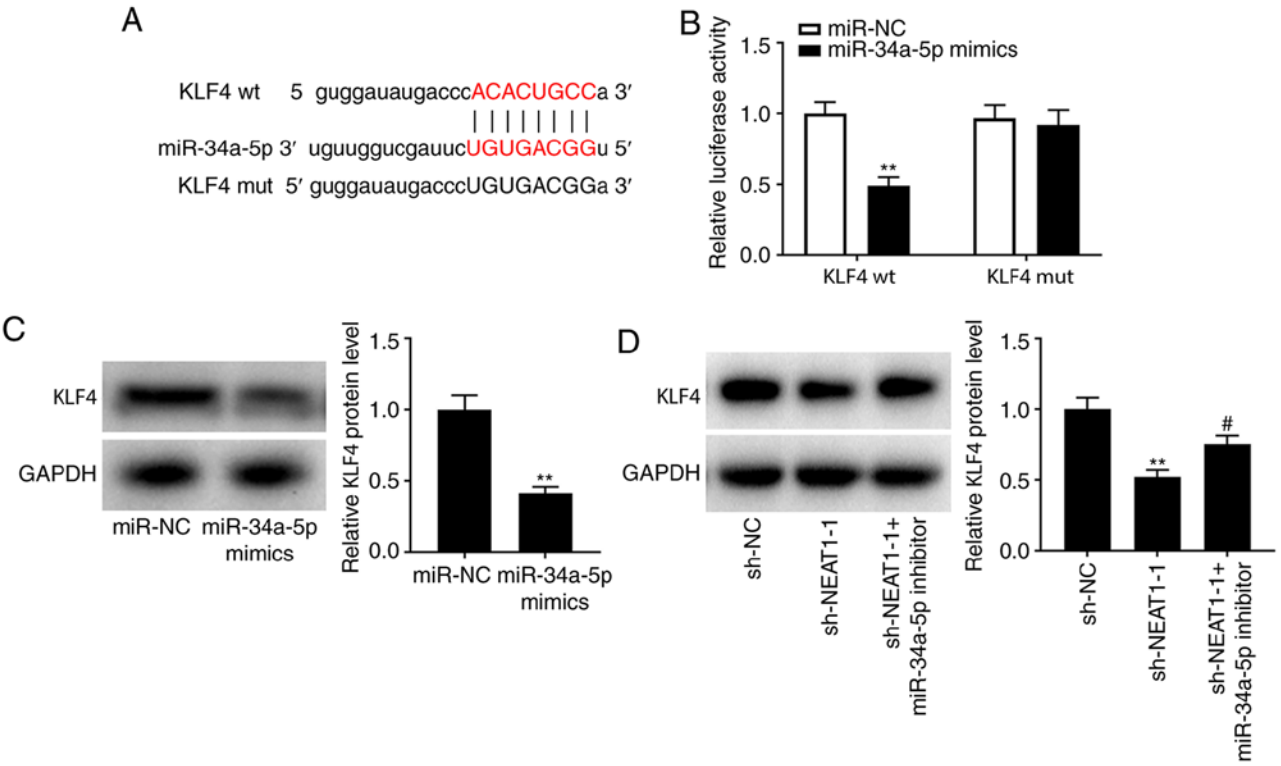

Figure 4. MiR-34a-5p targets KLF4. (A) The complementary binding site of NEAT1 and miR-34a-5p was predicted by TargetScan software. (B) The luciferase activity in PASMCs co-transfected with pGL3-KLF4 wt/pGL3-KLF4 mut and miR-34a-5p mimics/NC was determined by dual luciferase reporter assay. **P<0.01 vs. the miR-NC group. (C) The protein level of KLF4 in hypoxia-induced PASMCs after transfection of miR-34a-5p mimics/NC was detected by western blotting. **P<0.01 vs. the miR-NC group. (D) The protein level of KLF4 in hypoxia-induced PASMCs after transfection of sh-NEAT1-1/sh-NEAT1-1 + miR-34a-5p inhibitor was detected by western blotting. **P<0.01 vs. the sh-NC group; $^{\#}$P<0.01 vs. the sh-NEAT1-1 group. miR-34a-5p, microRNA-34a-5p; KLF4, Krüppel-like factor 4; NEAT1, nuclear paraspeckle assembly transcript 1; PASMCs, pulmonary arterial smooth muscle cells; wt, wild-type; mut, mutated; NC, negative control; sh-, short hairpin.

these transfected cells, feedback verification experiments were performed to further explore the regulatory mechanism involving NEAT1, miR-34a-5p, and KLF4 in PAH progression *in vitro*. The MTT, Transwell, and western blot assays revealed that under hypoxia, transfection of miR-34a-5p inhibitor and pcDNA-KLF4 partly eliminated the inhibitory effects of sh-NEAT1-1 on the proliferation and migration of PASMCs (Fig. 5C-E; P<0.05). The role of the NEAT1/miR-34a-5p/KLF4 axis in PASMC phenotype conversion and apoptosis was then further explored. As revealed in Fig. 5F, both low miR-34a-5p expression and high KLF4 expression reversed the promoting effects of NEAT1 downregulation on α-SMA level and the ratio of c-caspase-3/t-caspase-3 (P<0.01).

NEAT1 expression is upregulated in the serum of patients with PAH. To investigate the roles of NEAT1, miR-34a-5p, and KLF4 in PAH, their expression levels were assessed in the serum of patients with PAH. As revealed in Fig. 6A-C, in comparison to healthy volunteers, the expression levels of NEAT1 and KLF4 were significantly increased in the serum of patients with PAH, whereas miR-34a-5p expression was decreased (P<0.01). Additionally, there was a significant negative correlation between miR-34a-5p and NEAT1 (Fig. 6D; P=0.0052, r=-0.5408) as well as between miR-34a-5p and KLF4 (Fig. 6E; P=0.0041, r=-0.5536), whereas a significant positive correlation was observed between NEAT1 and KLF4 (Fig. 6F; P=0.0077, r=0.5197).

Discussion

PAH is a cardiovascular disease with a high mortality rate that is characterised by aberrant function of PASMCs (18,30). Sun *et al* analysed a microarray of lncRNAs in a rat model of PAH, and revealed that several lncRNAs were overexpressed (31). In addition, numerous previous studies have revealed several lncRNAs that are highly expressed in PAH, such as HOXA-AS3 (7), MALAT1 (8) and TUG1 (9). Consistently, in the present study it was revealed that NEAT1 expression was increased not only in hypoxia-treated PASMCs but also in the serum of patients with PAH. This result suggested that NEAT1 may be a pathogenetic lncRNA involved in the progression of PAH.

sh-NEAT1 was transfected into hypoxia-treated PASMCs to explore the possible role of NEAT1 in PAH progression *in vitro*. Notably, it was revealed that under hypoxic conditions, downregulation of NEAT1 markedly inhibited the proliferation and migration of PASMCs. Our results are in line with data from previous studies showing that aberrantly expressed NEAT1 had significant effects on lung-related diseases (32-36). In addition, it has been revealed that downregulation of NEAT1 suppressed cell proliferation, migration, and invasion in lung cancer (32-34), and NEAT1 overexpression aggravated inflammation and decreased lung function in asthma (35) and chronic obstructive pulmonary disease (36). It was hypothesized that knockdown

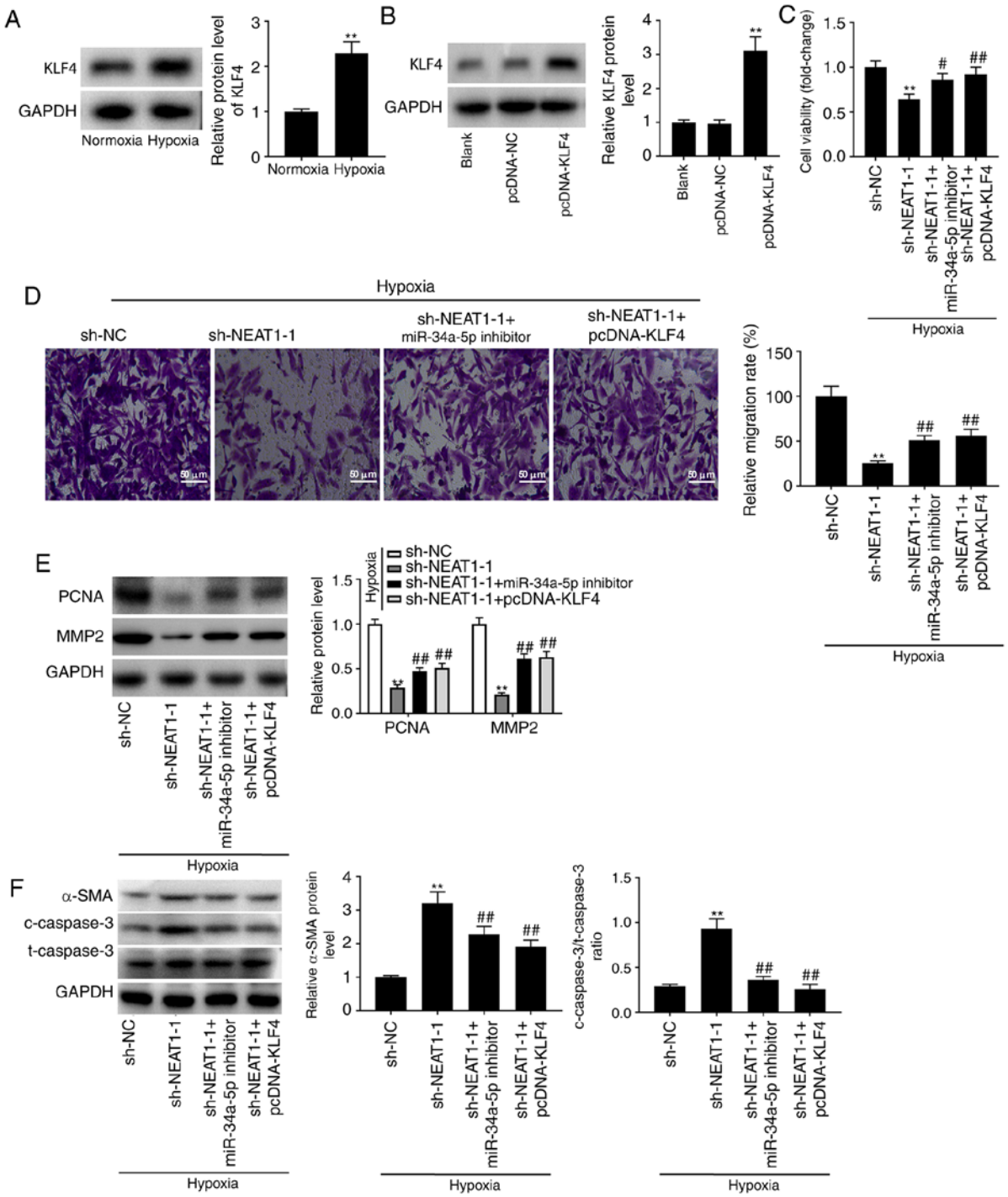

Figure 5. Knockdown of NEAT1 slows the process of PAH via sponging miR-34a-5p and downregulating KLF4. (A) The protein level of KLF4 in hypoxia-induced PASMCs was determined by western blotting. **P<0.01 vs. the normoxia PASMC group. (B) The protein level of KLF4 in hypoxia-induced PASMCs after transfection of pcDNA-KLF4/NC was determined by western blotting. **P<0.01 vs. the pcDNA-NC group. (C) The viability (OD_{450}) of hypoxia-induced PASMCs was measured by MTT assay. (D) The migration of hypoxia-induced PASMCs was measured by Transwell assay. Scale bar, 50 μm. (E) The protein levels of PCNA and MMP2 in hypoxia-induced PASMCs after transfection of sh-NEAT1-1/sh-NEAT1-1 + miR-34a-5p inhibitor/sh-NEAT1-1 + pcDNA-KLF4 were detected by western blotting. (F) The protein levels of α-SMA, and c-caspase-3/t-caspase-3 ratio in hypoxia-induced PASMCs after transfection of sh-NEAT1-1/sh-NEAT1-1 + miR-34a-5p inhibitor/sh-NEAT1-1 + pcDNA-KLF4 were detected by western blotting. **P<0.01 vs. the hypoxia + sh-NC group; $^{\#}$P<0.05, $^{\#\#}$P<0.01 vs. the hypoxia + sh-NC group. NEAT1, nuclear paraspeckle assembly transcript 1; PAH, pulmonary arterial hypertension; KLF4, Krüppel-like factor 4; PASMCs, pulmonary arterial smooth muscle cells; NC, negative control; MTT, 3-(4,5-dimethyl-2-thiazolyl)-2, 5-diphenyl-2-h-tetrazolium bromide; sh-, short hairpin; miR-34a-5p, microRNA-34a-5p; c-, cleaved; t-, total.

of NEAT1 may also inhibit hyperproliferation of the PA, thereby accelerating the progression of PAH. Transfection of si-NEAT1 was shown to inhibit the proliferation and migration of vascular smooth muscle cells (14). Given the inhibitory effects of NEAT1 silencing on the proliferation and migration of several types of human cancers (10-13), it was concluded that NEAT1 downregulation attenuates the progression of PAH *in vitro*.

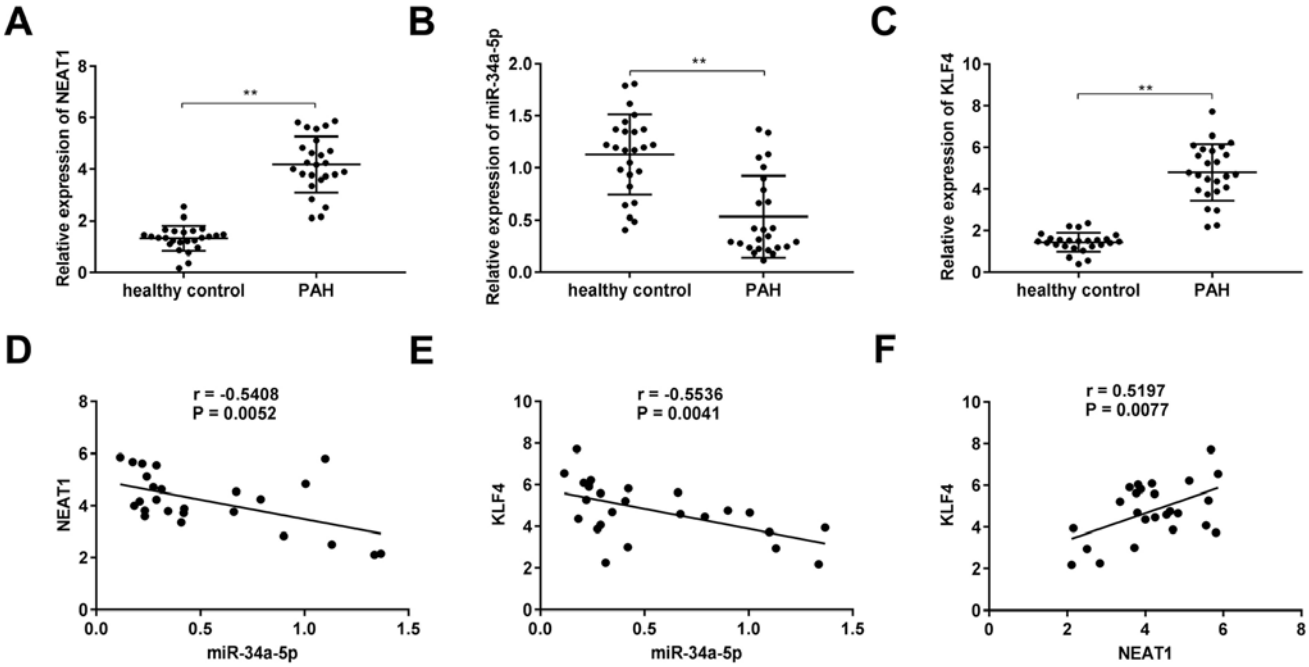

Figure 6. Upregulation of NEAT1 is revealed in the serum of patients with PAH. (A) The expression of NEAT1 in the serum of PAH patients (n=25) and the serum of healthy volunteers (n=25) was detected by RT-qPCR. **P<0.01. (B) The expression of miR-34a-5p in the serum of PAH patients (n=25) and the serum of healthy volunteers (n=25) was detected by RT-qPCR. **P<0.01. (C) The expression of KLF4 in the serum of PAH patients (n=25) and the serum of healthy volunteers (n=25) was detected by RT-qPCR. **P<0.01. (D) The correlation between the expression of NEAT1 and miR-34a-5p in the serum of PAH patients. P=0.0052, r=-0.5408. (E) The correlation between the expression of miR-34a-5p and KLF4 in the serum of PAH patients. P=0.0041, r=-0.5536. (F) The correlation between the expression of NEAT1 and KLF4 in the serum of PAH patients. P=0.0077, r=0.5197. NEAT1, nuclear paraspeckle assembly transcript 1; PAH, pulmonary arterial hypertension; miR-34a-5p, microRNA-34a-5p; KLF4, Krüppel-like factor 4; RT-qPCR, reverse transcription-quantitative PCR.

Over the past decade, several researchers have identified miRNAs with decreased expression levels in a rat model of PAH and PASMCs, including miR-98 (16), miR-140-5p (16), miR-106b-5p (37) and miR-124-3p (8). Similarly, in the present study, a reduction in the expression of miR-34a-5p in hypoxia-treated PASMCs and PAH patient serum was also revealed. Aberrant expression (especially overexpression) of miR-34a-5p has been shown to inhibit the malignant behaviours of pulmonary cancers and acute lung injury (38,39), and high miR-34a-5p expression inhibited cell proliferation, migration, and invasion in lung adenocarcinoma (38) and non-small cell lung cancer (39). In the present study, it was revealed that cell viability was reduced by transfection with miR-34a-5p mimics. Data from a recent study conducted by Wang *et al* are in line with our results: That upregulation of miR-34a reduced the proliferation of PASMCs (40). It was further demonstrated that miR-34a-5p plays an important role in suppressing cell migration and decreasing PCNA and MMP2 protein levels. Binding of NEAT1 and miR-34a-5p was predicted and confirmed in the present study. Therefore, it was predicted that the effect of miR-34a-5p on hyperplasia of PASMCs is modulated by NEAT1. To verify this, it was assessed whether NEAT1 can interact with miR-34a-5p, and the results revealed that transfection of a miR-34a-5p inhibitor reversed the suppressive effects of sh-NEAT1 on cell proliferation and migration. It was also revealed that miR-34a-5p expression was inversely correlated with NEAT1 expression. These results indicated that NEAT1 knockdown alleviates the development of PAH by upregulating miR-34a.

Deletion of KLF4 in smooth muscle protects against vascular diseases, such as aortic aneurysm and atherosclerosis (41,42). Notably, expression of KLF4 was shown to be elevated in both PAH model rats and patients (43,44). Consistently, it was determined that KLF4 was not only highly expressed in the serum of PAH patients but also in hypoxia-treated PASMCs. Given the positive correlation between KLF4 and NEAT1 in the serum of PAH patients and the targeting relationship between KLF4 and miR-34a-5p, it was hypothesized that KLF4 is also involved in PAH. The feedback verification experiments demonstrated that in hypoxia-treated PASMCs, transfection of pcDNA-KLF4 markedly reversed the inhibitory effects of sh-NEAT1 on cell proliferation and migration, which supported our hypothesis. In conclusion, the present results indicated that NEAT1 silencing alleviates PAH by regulating miR-34a-5p/KLF4.

However, there may be some limitations in this study. First, the expression of NEAT1 was only determined in PAH patients, and further detection of NEAT1 expression in patients with remission of PAH may be more scientific. Second, this study only focused on the cellular level, and more *in vivo* experiments are required. These issues will be elucidated in future studies.

In summary, the present results revealed that NEAT1 expression was increased in the serum of PAH patients and hypoxia-treated PASMCs. NEAT1 silencing attenuated PAH progression by upregulating miR-34a-5p and targeting KLF4. Our data provide a potential novel target and biomarker for the treatment or diagnosis of PAH.

Acknowledgements

Not applicable.

Funding

No funding was received.

Availability of data and materials

The datasets used and/or analyzed during the current study are available from the corresponding author on reasonable request.

Authors' contributions

XD and YM designed and analysed the data obtained from the experiments and were major contributors in writing the manuscript. XD and YM confirm the authenticity of all the raw data. YQ and QD performed the experiments and helped draft the manuscript. SZ, RT, and MP assisted in the experiments and revision of the manuscript. All authors read and approved the final manuscript.

Ethics approval and consent to participate

The present study was approved by the Ethics Committee of The People's Hospital of Rizhao (Rizhao, China). Written informed consent was obtained from all subjects.

Patient consent for publication

Not applicable.

Competing interests

The authors declare that they have no competing interests.

References

1. Hu W and Huang Y: Targeting the platelet-derived growth factor signalling in cardiovascular disease. Clin Exp Pharmacol Physiol 42: 1221-1224, 2015.
2. Lai YC, Potoka KC, Champion HC, Mora AL and Gladwin MT: Pulmonary arterial hypertension: The clinical syndrome. Circ Res 115: 115-130, 2014.
3. Gomez D and Owens GK: Smooth muscle cell phenotypic switching in atherosclerosis. Cardiovasc Res 95: 156-164, 2012.
4. Nie X, Chen Y, Tan J, Dai Y, Mao W, Qin G, Ye S, Sun J, Yang Z and Chen J: MicroRNA-221-3p promotes pulmonary artery smooth muscle cells proliferation by targeting AXIN2 during pulmonary arterial hypertension. Vascul Pharmacol 116: 24-35, 2019.
5. Lu X, Murphy TC, Nanes MS and Hart CM: PPAR{gamma} regulates hypoxia-induced Nox4 expression in human pulmonary artery smooth muscle cells through NF-{kappa}B. Am J Physiol Lung Cell Mol Physiol 299: L559-L566, 2010.
6. Shimoda LA and Laurie SS: Vascular remodeling in pulmonary hypertension. J Mol Med (Berl) 91: 297-309, 2013.
7. Zhang H, Liu Y, Yan L, Wang S, Zhang M, Ma C, Zheng X, Chen H and Zhu D: Long noncoding RNA Hoxaas3 contributes to hypoxia-induced pulmonary artery smooth muscle cell proliferation. Cardiovasc Res 115: 647-657, 2019.
8. Wang D, Xu H, Wu B, Jiang S, Pan H, Wang R and Chen J: Long noncoding RNA MALAT1 sponges miR1243p.1/KLF5 to promote pulmonary vascular remodeling and cell cycle progression of pulmonary artery hypertension. Int J Mol Med 44: 871-884, 2019.
9. Yang L, Liang H, Shen L, Guan Z and Meng X: lncRNA Tug1 involves in the pulmonary vascular remodeling in mice with hypoxic pulmonary hypertension via the microRNA-374c-mediated Foxc1. Life Sci 237: 116769, 2019.
10. Feng Y, Gao L, Cui G and Cao Y: lncRNA NEAT1 facilitates pancreatic cancer growth and metastasis through stabilizing ELF3 mRNA. Am J Cancer Res 10: 237-248, 2020.
11. Yan L, Zhang Z, Yin X and Li Y: lncRNA NEAT1 facilitates cell proliferation, invasion and migration by regulating CBX7 and RTCB in breast cancer. Onco Targets Ther 13: 2449-2458, 2020.
12. Chen LM, Niu YD, Xiao M, Li XJ and Lin H: lncRNA NEAT1 regulated cell proliferation, invasion, migration and apoptosis by targeting has-miR-376b-3p/SULF1 axis in non-small cell lung cancer. Eur Rev Med Pharmacol Sci 24: 4810-4821, 2020.
13. Wang S, Du H and Sun P: Long noncoding RNA NEAT1 contributes to the tumorigenesis of colorectal cancer through regulating SLC38A1 expression by sponging miR-138. Cancer Biother Radiopharm: Jul 17, 2020 (Epub ahead of print). doi: 10.1089/cbr.2020.3608.
14. Ahmed ASI, Dong K, Liu J, Wen T, Yu L, Xu F, Kang X, Osman I, Hu G, Bunting KM, *et al*: Long noncoding RNA NEAT1 (nuclear paraspeckle assembly transcript 1) is critical for phenotypic switching of vascular smooth muscle cells. Proc Natl Acad Sci USA 115: E8660-E8667, 2018.
15. Li Q, Zhou X and Zhou X: Downregulation of miR98 contributes to hypoxic pulmonary hypertension by targeting ALK1. Mol Med Rep 20: 2167-2176, 2019.
16. Zhu TT, Zhang WF, Yin YL, Liu YH, Song P, Xu J, Zhang MX and Li P: MicroRNA-140-5p targeting tumor necrosis factor-alpha prevents pulmonary arterial hypertension. J Cell Physiol 234: 9535-9550, 2019.
17. Sun L, Lin P, Chen Y, Yu H, Ren S, Wang J, Zhao L and Du G: miR-182-3p/Myadm contribute to pulmonary artery hypertension vascular remodeling via a KLF4/p21-dependent mechanism. Theranostics 10: 5581-5599, 2020.
18. Humbert M, Sitbon O and Simonneau G: Treatment of pulmonary arterial hypertension. N Engl J Med 351: 1425-1436, 2004.
19. Ghaleb AM and Yang VW: Kruppel-like factor 4 (KLF4): What we currently know. Gene 611: 27-37, 2017.
20. Sun D, Li Q, Ding D, Li X, Xie M, Xu Y and Liu X: Role of Kruppel-like factor 4 in cigarette smoke-induced pulmonary vascular remodeling. Am J Transl Res 10: 581-591, 2018.
21. Liang S, Yu H, Chen X, Shen T, Cui Z, Si G, Zhang JT, Cheng Y, Jia S, Song S, *et al*: PDGF-BB/KLF4/VEGF signaling axis in pulmonary artery endothelial cell angiogenesis. Cell Physiol Biochem 41: 2333-2349, 2017.
22. Feng F, Liu H, Chen A, Xia Q, Zhao Y, Jin X and Huang J: miR-148-3p and miR-152-3p synergistically regulate prostate cancer progression via repressing KLF4. J Cell Biochem 120: 17228-17239, 2019.
23. Zhao L, Han T, Li Y, Sun J, Zhang S, Liu Y, Shan B, Zheng D and Shi J: The lncRNA SNHG5/miR-32 axis regulates gastric cancer cell proliferation and migration by targeting KLF4. FASEB J 31: 893-903, 2017.
24. Zhai F, Cao C, Zhang L and Zhang J: miR-543 promotes colorectal cancer proliferation and metastasis by targeting KLF4. Oncotarget 8: 59246-59256, 2017.
25. Livak KJ and Schmittgen TD: Analysis of relative gene expression data using real-time quantitative PCR and the 2(-Delta Delta C(T)) method. Methods 25: 402-408, 2001.
26. Cardano M, Tribioli C and Prosperi E: Targeting proliferating cell nuclear antigen (PCNA) as an effective strategy to inhibit tumor cell proliferation. Curr Cancer Drug Targets 20: 240-252, 2020.
27. Wu DM, Deng SH, Liu T, Han R, Zhang T and Xu Y: TGF-β-mediated exosomal lnc-MMP2-2 regulates migration and invasion of lung cancer cells to the vasculature by promoting MMP2 expression. Cancer Med 7: 5118-5129, 2018.
28. Xu MM, Deng HY and Li HH: MicroRNA-27a regulates angiotensin II-induced vascular smooth muscle cell proliferation and migration by targeting α-smooth muscle-actin in vitro. Biochem Biophys Res Commun 509: 973-977, 2019.
29. Shi S, Liu XL and Li HB: Downregulation of caspase-3 alleviates mycoplasma pneumoniae-induced apoptosis in alveolar epithelial cells. Mol Med Rep 16: 9601-9606, 2017.
30. Archer SL, Weir EK and Wilkins MR: Basic science of pulmonary arterial hypertension for clinicians: New concepts and experimental therapies. Circulation 121: 2045-2066, 2010.

31. Sun Z, Liu Y, Yu F, Xu Y, Yanli L and Liu N: Long non-coding RNA and mRNA profile analysis of metformin to reverse the pulmonary hypertension vascular remodeling induced by monocrotaline. Biomed Pharmacother 115: 108933, 2019.
32. Qi L, Liu F, Zhang F, Zhang S, Lv LY, Bi Y and Yu Y: lncRNA NEAT1 competes against let-7a to contribute to non-small cell lung cancer proliferation and metastasis. Biomed Pharmacother 103: 1507-1515, 2018.
33. Yu PF, Wang Y, Lv W, Kou D, Hu HL, Guo SS and Zhao YJ: lncRNA NEAT1/miR-1224/KLF3 contributes to cell proliferation, apoptosis and invasion in lung cancer. Eur Rev Med Pharmacol Sci 23: 8403-8410, 2019.
34. Ma F, Lei YY, Ding MG, Luo LH, Xie YC and Liu XL: lncRNA NEAT1 interacted with DNMT1 to regulate malignant phenotype of cancer cell and cytotoxic T cell infiltration via epigenetic inhibition of p53, cGAS, and STING in lung cancer. Front Genet 11: 250, 2020.
35. Li X, Ye S and Lu Y: Long non-coding RNA NEAT1 overexpression associates with increased exacerbation risk, severity, and inflammation, as well as decreased lung function through the interaction with microRNA-124 in asthma. J Clin Lab Anal 34: e23023, 2020.
36. Ming X, Duan W and Yi W: Long non-coding RNA NEAT1 predicts elevated chronic obstructive pulmonary disease (COPD) susceptibility and acute exacerbation risk, and correlates with higher disease severity, inflammation, and lower miR-193a in COPD patients. Int J Clin Exp Pathol 12: 2837-2848, 2019.
37. Chen H, Ma Q, Zhang J, Meng Y, Pan L and Tian H: miR-106b-5p modulates acute pulmonary embolism via NOR1 in pulmonary artery smooth muscle cells. Int J Mol Med 45: 1525-1533, 2020.
38. Li W, Pan T, Jiang W and Zhao H: HCG18/miR-34a-5p/HMMR axis accelerates the progression of lung adenocarcinoma. Biomed Pharmacother 129: 110217, 2020.
39. Luo S, Shen M, Chen H, Li W and Chen C: Long noncoding RNA TP73AS1 accelerates the progression and cisplatin resistance of nonsmall cell lung cancer by upregulating the expression of TRIM29 via competitively targeting microRNA34a5p. Mol Med Rep 22: 3822-3832, 2020.
40. Wang P, Xu J, Hou Z, Wang F, Song Y, Wang J, Zhu H and Jin H: miRNA-34a promotes proliferation of human pulmonary artery smooth muscle cells by targeting PDGFRA. Cell Prolif 49: 484-493, 2016.
41. Shankman LS, Gomez D, Cherepanova OA, Salmon M, Alencar GF, Haskins RM, Swiatlowska P, Newman AA, Greene ES, Straub AC, *et al*: KLF4-dependent phenotypic modulation of smooth muscle cells has a key role in atherosclerotic plaque pathogenesis. Nat Med 21: 628-637, 2015.
42. Salmon M, Johnston WF, Woo A, Pope NH, Su G, Upchurch GR Jr, Owens GK and Ailawadi G: KLF4 regulates abdominal aortic aneurysm morphology and deletion attenuates aneurysm formation. Circulation 128 (11 Suppl 1): S163-S174, 2013.
43. Sheikh AQ, Misra A, Rosas IO, Adams RH and Greif DM: Smooth muscle cell progenitors are primed to muscularize in pulmonary hypertension. Sci Transl Med 7: 308ra159, 2015.
44. Sheikh AQ, Saddouk FZ, Ntokou A, Mazurek R and Greif DM: Cell autonomous and non-cell autonomous regulation of SMC progenitors in pulmonary hypertension. Cell Rep 23: 1152-1165, 2018.